Molecular Therapy
Nucleic Acids
Original Article

# A non-viral and selection-free *COL7A1* HDR approach with improved safety profile for dystrophic epidermolysis bullosa

Thomas Kocher,[1] Johannes Bischof,[1] Simone Alexandra Haas,[2,3] Oliver Patrick March,[1] Bernadette Liemberger,[1] Stefan Hainzl,[1] Julia Illmer,[1] Anna Hoog,[4] Katharina Muigg,[4] Heide-Marie Binder,[4] Alfred Klausegger,[1] Dirk Strunk,[4] Johann Wolfgang Bauer,[1,5] Toni Cathomen,[2,3,6] and Ulrich Koller[1]

[1]EB House Austria, Research Program for Molecular Therapy of Genodermatoses, Department of Dermatology and Allergology, University Hospital of the Paracelsus Medical University Salzburg, 5020 Salzburg, Austria; [2]Institute for Transfusion Medicine and Gene Therapy, Medical Center – University of Freiburg, 79106 Freiburg, Germany; [3]Center for Chronic Immunodeficiency, Medical Center – University of Freiburg, 79106 Freiburg, Germany; [4]Cell Therapy Institute, SCI-TReCS, Paracelsus Medical University, 5020 Salzburg, Austria; [5]Department of Dermatology and Allergology, University Hospital of the Paracelsus Medical University Salzburg, 5020 Salzburg, Austria; [6]Faculty of Medicine, University of Freiburg, 79106 Freiburg, Germany

**Gene editing via homology-directed repair (HDR) currently comprises the best strategy to obtain perfect corrections for pathogenic mutations of monogenic diseases, such as the severe recessive dystrophic form of the blistering skin disease epidermolysis bullosa (RDEB). Limitations of this strategy, in particular low efficiencies and off-target effects, hinder progress toward clinical applications. However, the severity of RDEB necessitates the development of efficient and safe gene-editing therapies based on perfect repair. To this end, we sought to assess the corrective efficiencies following optimal Cas9 nuclease and nickase-based *COL7A1*-targeting strategies in combination with single- or double-stranded donor templates for HDR at the *COL7A1* mutation site. We achieved HDR-mediated correction efficiencies of up to 21% and 10% in primary RDEB keratinocytes and fibroblasts, respectively, as analyzed by next-generation sequencing, leading to full-length type VII collagen restoration and accurate deposition within engineered three-dimensional (3D) skin equivalents (SEs). Extensive on- and off-target analyses confirmed that the combined treatment of paired nicking and single-stranded oligonucleotides constituted a highly efficient *COL7A1*-editing strategy, associated with a significantly improved safety profile. Our findings, therefore, represent a further advancement in the field of traceless genome editing for genodermatoses.**

## INTRODUCTION

Recessive dystrophic epidermolysis bullosa (RDEB) is a rare, though severe, inherited skin disorder caused by mutations in the *COL7A1* gene, resulting in compromised type VII collagen (C7) protein function.[1] C7 is an important constituent and stabilizer of dermal-epidermal adhesion at the basement membrane zone (BMZ), forming anchoring fibrils (AFs) beneath the lamina densa. In RDEB patients, lack or loss of function of C7 AFs causes severe blistering of the skin and mucous membranes upon minor mechanical stress. Such trauma frequently leads to chronic open wounds, typically associated with severe clinical complications—including aggressive squamous cell carcinoma (SCC).[1–3] While open wounds significantly affect a patient's quality of life from birth, SCCs arise in early adulthood and cause patient mortality.[3] There is currently no specific treatment available for RDEB, and clinical approaches mainly focus on temporary symptom alleviation, underlining the urgent need for efficient and safe therapeutic approaches.

Two useful forms of gene therapy are currently feasible for EB: gene replacement and genome editing.[4,5] In recent years, gene replacement approaches have been successfully applied to treat LAMB3-deficient junctional EB patients.[4,6,7] However, initial attempts to stably integrate *COL7A1* cDNA into RDEB patient cell genomes have yielded limited therapeutic success so far.[8] This limitation might be due to low viral transduction efficiencies, random transgene integrations, and unwanted genomic recombinations.[8–10] Thus, targeting C7-deficient patient cells via designer nucleases presents a possibility of circumventing many of these issues. Further, gene editing is suitable to correct dominantly and recessively inherited mutations, as recently demonstrated.[5]

Clustered Regularly Interspaced Short Palindromic Repeats (CRISPR)-CRISPR-associated protein 9 (Cas9)-mediated gene editing relies on the simultaneous delivery of a Cas9 nuclease and a target-specific single-guide RNA (sgRNA) into the target cells, thereby enabling precise, sequence-specific editing. However, the efficient and accurate correction of EB-related genes is critically reliant on the prior definition of

Received 14 December 2020; accepted 25 May 2021;
https://doi.org/10.1016/j.omtn.2021.05.015.

**Correspondence:** Ulrich Koller, EB House Austria, Research Program for Molecular Therapy of Genodermatoses, Department of Dermatology and Allergology, University Hospital of the Paracelsus Medical University Salzburg, Strubergasse 22, 5020 Salzburg, Austria.
**E-mail:** u.koller@salk.at

an effective, specific targeting strategy. Each targeting strategy relies on DNA cleavage and the subsequent induction of naturally occurring repair pathways in the cell, implicated in repairing genome-editing-induced double-strand breaks (DSBs).[5] The majority of DSBs are repaired via either the classical end-joining (c-EJ) pathway, also known as non-homologous end-joining (NHEJ), involving the direct ligation of the two DNA ends perfectly, or the error-prone alternative EJ pathway if classical EJ fails to repair the DSB.[11,12] Besides EJ pathways, homology-directed repair (HDR) can occur when a homologous donor sequence is provided comprising either a double- or single-stranded DNA template almost homologous to the targeted area.[13]

Currently, the most straightforward and efficient strategies for *COL7A1* editing are based on EJ-mediated gene disruption, gene reframing, and exon deletion.[14–20] These approaches rely on introducing insertions and deletions (indels) at the target loci, mainly resulting in a broad heterogeneity of repair outcomes. Wu et al.[19] and Bonafont et al.[20] described exon deletion-based reframing strategies with homogeneous editing outcomes to treat hotspot mutations in exon 80 of *COL7A1*. Recently, Kocher et al.[18] demonstrated efficient and predictable CRISPR-Cas9-mediated gene reframing in primary keratinocytes. This approach minimized the unwanted heterogeneity of repair outcomes, which likely result in non-functional C7 variants. The dominant repair outcome was a precise single adenine sense-strand insertion, which resulted in a single amino-acid divergence from the wild-type coding sequence.

However, a highly efficient and safe method to achieve perfect wild-type sequence restoration, applicable for a significant portion of disease-causing mutations, remains the ultimate goal of gene editing. HDR-based approaches, together with novel technologies, such as base editing and prime editing, can lead to precise correction of pathogenic gene mutations.[21–23] However, a caveat of HDR approaches for the seamless repair of RDEB keratinocytes and fibroblasts is the generally low efficiency. This often necessitates the use of selection to enrich for corrected cells. Most HDR-based RDEB studies include pre-selection steps of cells in bulk, limited dilutions, clonal selections, single-cell expansions, and screening for edited clones.[13,24–30] Many other strategies require the introduction of selection cassettes, which, after Cre-mediated removal, leave a loxP footprint and cannot be considered traceless.[15,24–27] Strategies involving plasmid-based delivery and selection-based strategies are often accompanied by a high risk of off-target effects due to prolonged nuclease expression and targeted or random integration of the entire donor plasmid or large fragments.[13] Therefore, nuclease-mediated HDR requires optimization to achieve selection-free, precise, and traceless correction of *COL7A1* mutations at therapeutically relevant efficiencies.

The protein-based delivery of Cas9 molecules complexed with sgRNA (ribonucleoproteins, RNPs) can negate possible integrations of commonly used delivery vectors and has been shown to increase targeting efficiency compared to plasmid transfections.[18,20] Furthermore, electroporation is an effective and relatively nontoxic method of delivering these molecules *ex vivo*.[31] Further, the reduced time span of nuclease expression improves the safety profile significantly.[32] In addition, using a catalytically modified version of *Streptococcus pyogenes* (sp) Cas9 (Cas9), spCas9-D10A nickase (Cas9n), commercially available as protein, can considerably reduce the risk of unwanted off-target effects.[13,33–36] Using a pair of sgRNAs to guide two Cas9 nickases in close proximity on opposite strands and in correct orientation to a target locus enables the simultaneous generation of two nicks and thus mediates improved HDR outcomes.[35]

Here, we demonstrate the precise correction of a splice-site mutation in exon 3 of *COL7A1* in primary RDEB keratinocytes and fibroblasts using paired nickases and DNA oligonucleotides (Oligos) via HDR. We compared HDR efficiencies mediated by Cas9, Cas9n, and paired Cas9n approaches combined with either single-stranded oligonucleotides (ssOligos) or double-stranded oligonucleotides (dsOligos) with 5′ overhangs (5′OHOligos). As a result, approaches based on single Cas9 nucleases or paired Cas9n nickases combined with ssOligos consistently outperformed all other editing strategies when targeting *COL7A1*. Further, we investigated the effects of cold shock on target cells, confirming that transient 32°C treatment further improves the overall HDR efficiency.[37] Secretion of restored type VII collagen was observed in supernatants of treated primary keratinocytes and fibroblasts, resulting in correct C7 deposition in engineered three-dimensional (3D) skin equivalents (SEs). Extensive on- and off-target analyses in the course of this study revealed that the paired nicking strategy, featuring the most robust gene editing safety profile, also reduced the risk of unwanted on- and off-target repair template integrations within the genome of treated RDEB cells.

## RESULTS

### *COL7A1* editing strategy via HDR

Recently, we demonstrated that using the Cas9 D10A nickase variant (Cas9n) of *Streptococcus pyogenes* (sp) in combination with paired sgRNAs is a highly effective strategy for the HDR-based repair of a prevalent *COL7A1* mutation (c.425A>G) in RDEB keratinocytes.[13] We improved this plasmid-based approach, through the use of RNPs. These comprise sgRNA Cas9/Cas9n complexed proteins (RNPs) specifically targeting intron 3 of *COL7A1* (Figure 1). Electroporation of Cas9 RNPs includes a superior and safe method of delivering gene-editing agents into cells, associated with reduced off-target effects, absence of potentially recombinogenic exogenous DNA, higher rates of gene disruption, and a reduced window of activity.[18,20] Double-stranded (ds) DNA donor templates featuring 5′ overhangs have been demonstrated to result in almost 2-fold higher HDR efficiencies.[38] Consequently, we employed double-stranded oligonucleotides with overhangs and unannealed short single-stranded oligonucleotides as HDR templates (Figure 1). Wild-type Cas9 RNPs or paired Cas9n RNPs for double-nicking together with HDR templates were delivered into RDEB patient keratinocytes and fibroblasts via electroporation using the Neon transfection system.

### *COL7A1* editing in immortalized RDEB keratinocytes

Upon RNP delivery into immortalized RDEB223 keratinocytes (c.425A>G/c.425A>G), Cas9n-generated single-strand breaks (SSBs)

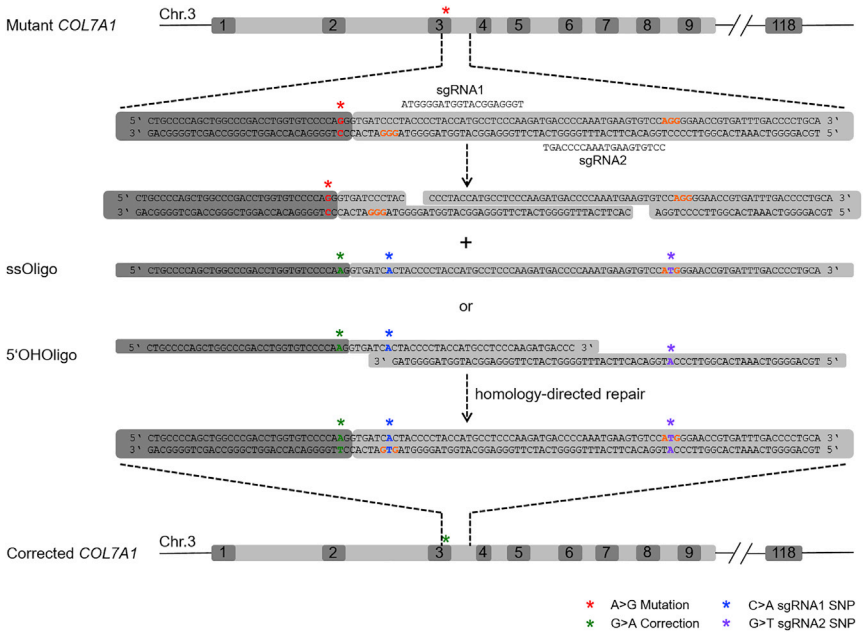


**Figure 1. Strategy design for HDR-based *COL7A1* repair**

Partial map of *COL7A1*, showing exons (dark gray boxes), introns (light gray boxes), and patient mutation (c.425A>G) (red asterisk) within exon 3 of *COL7A1*. Electroporation of Cas9 and Cas9n RNPs in double-nicking constellation leads to the induction of overhanging double-strand breaks (DSBs) within intron 3 of *COL7A1*, proximal to the patient mutation. Single- and double-stranded oligonucleotides with overhangs serve as HDR templates. Following induction of a DSB via RNPs, the HDR-based repair leads to the disruption of both PAM sites (orange) within intron 3 (blue and purple asterisks). Instances of optimal genome editing will result in a G to A exchange (green asterisk) at the mutation site, resulting in genotypic restoration within RDEB keratinocytes.

and Cas9-generated DSBs led to the induction of several DNA repair pathways. Our strategy of traceless HDR-mediated correction of the disease-associated mutation includes the introduction of SNPs (c.426+7C>A; c.626+52G>T) at selected protospacer adjacent motif (PAM) sites, precluding recurrent Cas9 targeting (Figure 2A). Keratinocytes treated with either Cas9/sgRNA1, Cas9/sgRNA2, or dual targeting of double-nicking Cas9n (Cas9n/sgRNA1 and Cas9n/sgRNA2), with or without repair templates, displayed an apparent propensity for EJ-based repair pathways, with indels observed in over 84% of next-generation sequencing (NGS)-analyzed *COL7A1* alleles (Figure 2B). There was a tendency for reduced indel formation with the addition of ssOligos and 5′OHOligos (Figure 2B). The majority of observed indels comprised deletions, typically occurring at the RNP targeting sites. Interestingly, the frequency of insertions at the target site increased with the co-delivery of 5′OHOligos, particularly when combining 5′OHOligos with Cas9 RNPs (Figure 2B). T7 endonuclease I (T7EI) assays confirmed the comparable and high targeting efficiencies for each strategy (Figure S1). When analyzing the resulting indels via NGS, we found similar size distribution patterns regardless of whether RNPs were delivered exclusively or concurrently with ssOligos or 5′OHOligos into the target cells (Figures S2–S4). We observed an increased frequency of insertions at the target site only in samples treated with Cas9/sgRNA1 in conjunction with 5′OHOligos. In these samples, size distribution analyses demonstrated a dominant 29–30 nt long insertion at the Cas9/sgRNA1 cutting site (Figure S4). This specific insertion was not detectable with any of the other strategies.

Co-delivery of DSB-generating nuclease with either single-stranded (ssOligos) or double-stranded (5′OHOligos) HDR templates into RDEB223 keratinocytes resulted in the repair of the mutation (c.425A>G) in 6.2%–7.9% of all analyzed *COL7A1* alleles (Figure 2C). As expected, this led to the restoration of C7 within corrected cells (Figures 2D and S5). Subsequent flow cytometric analysis indicated C7 restoration efficiencies of up to 14% of samples treated with the double-nicking approach and Cas9/sgRNA1 (Figure 2E). Improved correction efficiencies were not detected or observed via NGS, immunofluorescence (IF), or flow cytometric analyses in samples treated with nuclease and 5′OHOligos, compared to ssDNA templates (Figures 2C, 2E, S5, and S6).

Notably, a C7 restoration in up to 3.90% of exclusively Cas9/sgRNA- and paired Cas9n/gRNA-treated RDEB keratinocytes was detected via flow cytometric analysis (Figures 2E and S6) and confirmed via immunofluorescence staining (Figure S5). This might be due to EJ-induced indels at the *COL7A1* on-target site leading to the generation of in-frame C7 protein variants, differing partially in the amino acid sequence to the wild-type protein.

### Off-target analysis for *COL7A1* editing in immortalized RDEB keratinocytes reveals an improved safety profile for the ssOligo/double-nicking approach compared to 5′OHOligo- and Cas9-based approaches

Aside from the high on-target efficiency of RNPs, possible future clinical implementations must address several safety concerns. The most promising approaches regarding HDR and C7 restoration efficiencies were therefore analyzed for Cas9 nucleases/nickase off-target activity, off-target donor template integration, and on-target template integrations. These comprised Cas9/sgRNA1 and Cas9n/gRNA1+2 targeting with an ssOligo or 5′OHOligo HDR template. Off-target analysis of our previous plasmid-based approach highlighted the potential of RNA-guided engineered nucleases to cleave off-target sites that differ by several nucleotides from the on-target sites, leading to unwanted off-target mutations.[13] The dominant off-target site described within our recent study tolerated one RNA bulge and one mismatch. To confirm this high activity at this predicted off-target site in our updated, selection-free strategy, we analyzed isolated DNA of keratinocyte bulk populations treated with the respective RNPs. Initial T7EI

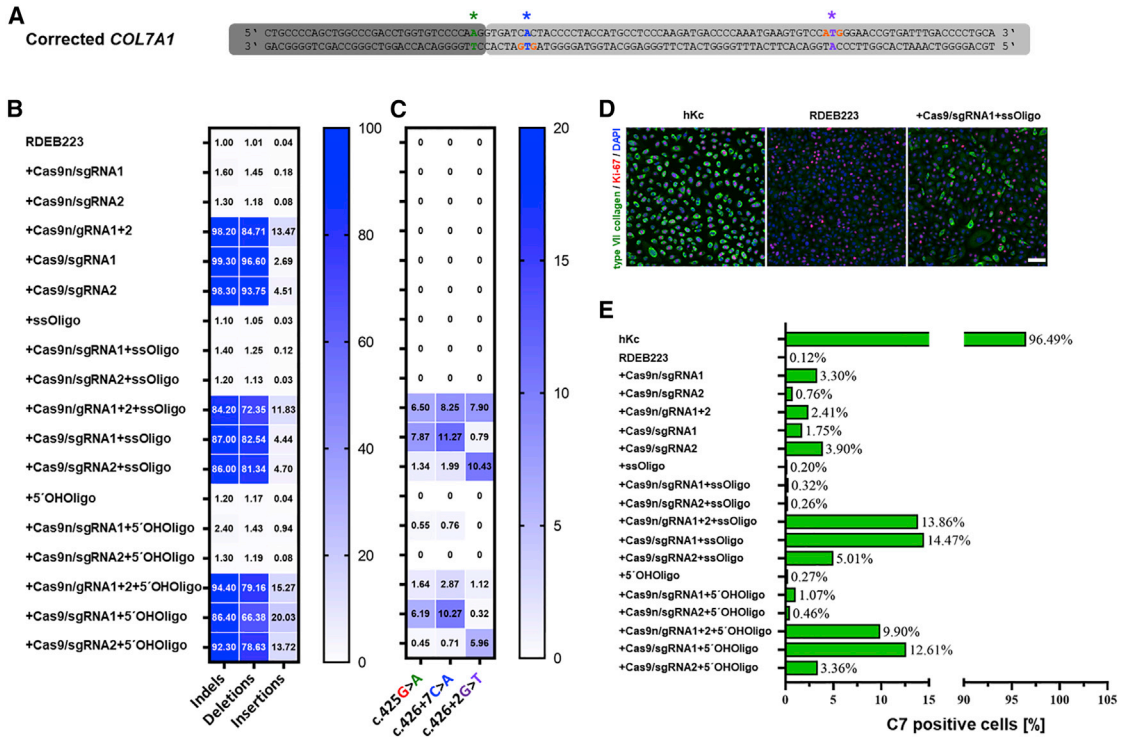


**Figure 2. *COL7A1* editing in immortalized RDEB keratinocytes**

(A) RNP-mediated SSBs and DSBs at the *COL7A1* targeting site activate EJ- and HDR-based repair pathways. In optimal instances, this results in correction of the disease-associated mutation in exon 3 (green asterisk) and disruption of the PAM sites (blue and purple asterisks) via HDR. (B) NGS analyses of the PCR-amplified *COL7A1* on-target site revealed high indel frequencies (84%–99%) in RDEB223 keratinocytes treated with Cas9/single-guide RNA (sgRNA1), Cas9/sgRNA2, and double nicking (Cas9n/sgRNA1 and Cas9n/sgRNA2). (C) Precise repair, analyzed via NGS, between the *COL7A1* on-target site and the respective repair template (ssOligo or 5′OHOligo) leads to correction of the disease-associated mutation (c.425A>G). This can occur irrespective of HDR-mediated editing of PAM sites (c.426+7C>A and c.426+52G>T). The frequency of these events is dependent upon the targeting and repair strategy. (D) Immunofluorescence staining revealed C7 restoration (AF488; green) within corrected RDEB223 keratinocytes treated with Cas9/sgRNA1 and ssOligos (scale bar, 100 μm). (E) Flow cytometric analyses on C7-stained, RNP-treated RDEB223 keratinocytes revealed the expression of C7 in 0.76%–3.90% of all analyzed cells. Strategies utilizing either ssOligos or 5′OHOligos to correct the mutation demonstrated increased levels of C7 restoration, up to 9.9%–14.47%.

assay analysis indicated robust targeting at the off-target site only in the Cas9/sgRNA1-treated sample (Figure S7). NGS analysis confirmed exceptionally high off-target site 7 (off7) targeting efficiencies of up to 96% for Cas9/sgRNA1-treated cells (Figure 3A); most edits comprised deletions. However, samples co-treated with Cas9/sgRNA1 and each of our templates demonstrated a markedly increased incidence of insertions (5.5% for Cas9, 7.3% with the addition of ssOligos, and ≥30% with the addition of 5′OHOligos) (Figures 3A and S7). This was not observed in any of the double-nicking-treated samples (Figure S8). Samples treated with Cas9/sgRNA1 and either repair template demonstrated a dominant 1 nt G insertion at off-target site 7, comprising ~38% and ~12% of total insertional NGS reads. However, samples co-treated with the 5′OHOligo template displayed extensive (~10%) off-target template insertions (Figures 3B and 3C). Similar insertions have been observed when analyzing the on-target site within the same sample (Figure S4). In contrast, ssOligo-treated samples largely displayed small off-target insertions (Figure 3C), indicating preferable use of ssOligos for HDR-mediated gene editing instead of dsOligos.

In addition to the previously characterized Cas9/sgRNA1 off-target site 7 (formerly described as OT9), we utilized Abnoba-Seq for *in vitro* identification of additional 12 sites for Cas9/sgRNA1 and Cas9/sgRNA2 of likely off-target activity (Table S1).[13,39] Subsequent NGS analyses of these loci revealed indel formations at five off-target sites in Cas9-treated samples (Figure 4), comprising mainly deletions (Figure S9). Of all Abnoba-Seq-identified loci, off6 appeared to represent the Cas9/sgRNA1 off-target with the greatest activity, with 0.38% of reads displaying indels. However, analysis of Cas9n- and double-nicking-treated patient keratinocytes identified no off-target editing, confirming the improved safety profile of double-nicking-based gene-editing strategies in comparison to Cas9 nuclease-based approaches.

### Temperature-mediated increase of correction efficiencies and HDR rates in immortalized RDEB keratinocytes

Several recent studies have sought to further improve HDR rates in mammalian cell types.[37,40–47] Pre- and post-exposure of nuclease-treated cells to 32°C has been shown to increase the HDR efficiencies

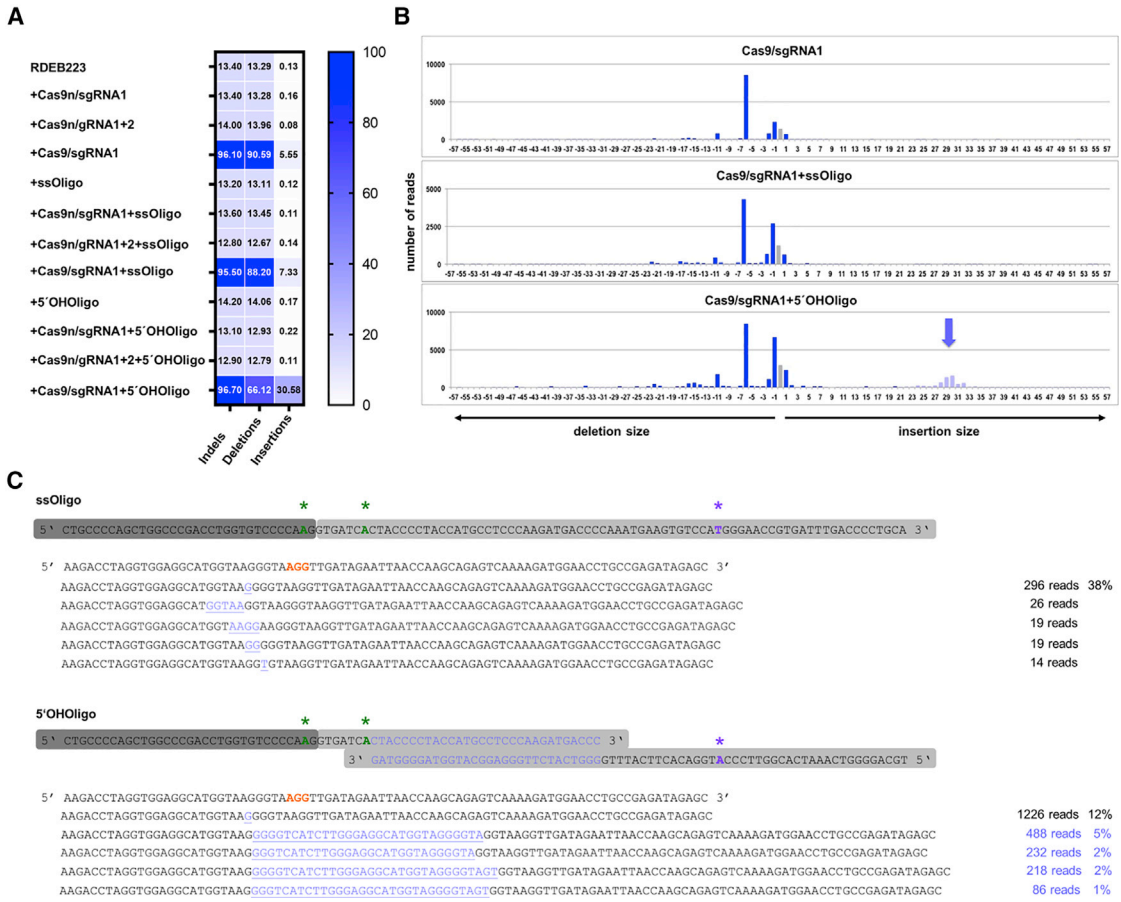


**Figure 3. Repair template integration at the previously characterized Cas9/sgRNA1 off-target site 7 (off7) (OT9)**

(A) NGS analyses of the PCR-amplified off-target site. Editing efficiencies are presented as heatmaps. (B) Size distribution diagram of NGS-analyzed off-target sequences. The arrow highlights the insertion/integration of a ~30 nt DNA fragment arising from the utilization of 5′OHOligos in our HDR approach. (C) Most prominent indel sequences and read numbers are listed for NGS-analyzed samples of Cas9/sgRNA1+ssOligos and Cas9/sgRNA1+5′OHOligo-treated RDEB223 keratinocyte bulk populations.

between 2- and 10-fold in cell types displaying low HDR rates at 37°C.[37] We investigated whether we could increase HDR rates following the implementation of our gene-editing strategies via a brief 32°C cold shock of patient keratinocytes before and after nucleofection. This would negate the use of cell cycle modulating reagents and small molecules, which have previously been shown to boost HDR rates. Their addition might increase the complexity of the approach and might cause undesirable side effects.[40,41] To ascertain the effect of cold shock on HDR rates, we analyzed our two most promising HDR strategies. To this end, we first nucleofected Cas9/sgRNA1 RNPs and Cas9n/gRNA1+2 RNPs together with ssOligos into cold-shocked keratinocytes. Following 24 h of transient hypothermic treatment, cells were shifted back to 37°C for 1 week. We determined the rates of NHEJ- and HDR-based DSB repair by targeted amplicon NGS, C7 restoration by immunofluorescence, and flow cytometric analysis of intracellular C7 (Figure 5). We observed slightly improved HDR frequencies following cold shock for both HDR strategies, compared to standard culture conditions (Figure 5B). Quantification of NHEJ events within RNP-treated samples and samples additionally treated with ssOligos revealed a clear decrease in the frequency of these unwanted events following co-treatment with the repair template (99.13% and 99.21% for RNPs; 90.93% and 88.26% for RNPs and ssOligos). This decrease was more pronounced following cold shock (98.60% and 99.40% for RNPs; 80.72% and 80.85% for RNPs and ssOligos) (Figure 5A). Analyses of C7 expression and restoration demonstrated slightly increased correction efficiencies for cold-shock-treated samples (Figures 5B, 5C, and S10). This temperature-induced increase in C7 restoration was more prominent in the Cas9n/gRNA1+2+ssOligo-treated sample than the Cas9/sgRNA1+ssOligo-treated sample (11.67% to 15.88% versus 8.76% to 9.13%) (Figures 5D and S10).

### HDR rates in primary RDEB keratinocytes

To confirm our safest and most efficient HDR strategy in a more clinically relevant setting, we nucleofected Cas9n/gRNA1+2 RNPs together with the ssOligos into primary patient-derived RDEB223 keratinocytes. These were subjected to cold shock pre- and post-nucleofection. T7EI assay indicated high RNP targeting efficiencies in treated primary

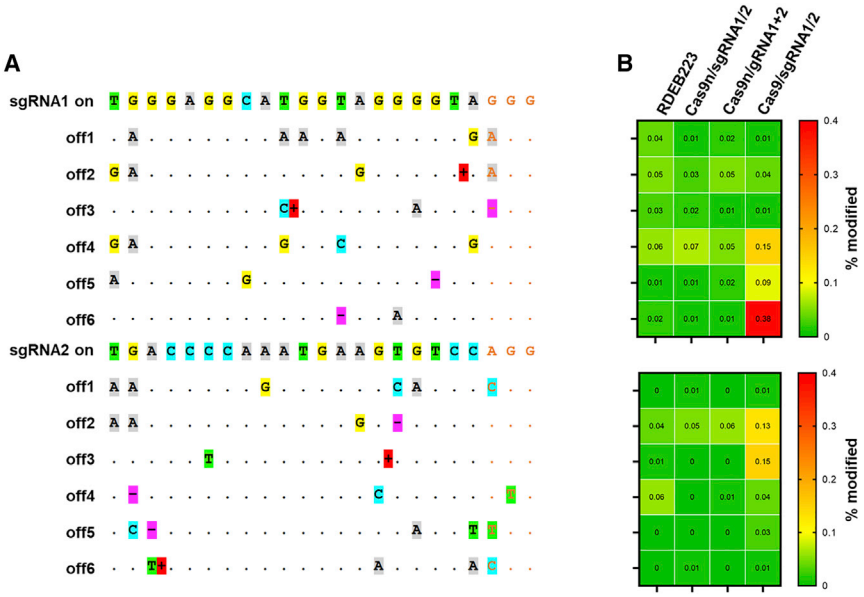


**Figure 4. NGS-based identification of off-target activity *in vitro***

(A) Off-target (off) sites for *COL7A1* intron 3-targeting sgRNAs 1 and 2. RDEB223 keratinocytes were transfected with Cas9n or Cas9 and sgRNAs. PCR amplification of off-target loci identified by Abnoba-Seq was performed on genomic DNA isolated 1 week after nucleofection. Purple boxes (–) correspond to RNA bulges, red boxes (+) indicate DNA bulges. Letters within colored boxes indicate mismatches between sgRNA and off-target binding region. Orange letters indicate the PAM sites. (B) Targeted amplicon NGS sequencing was subsequently performed. Detected indel frequencies are presented as heatmaps.

keratinocytes (Figure S11). NGS analysis of treated bulk populations revealed similar targeting efficiencies to those observed in the immortalized cell line, with indels present in 63.0% of analyzed reads (Figure 6A). Of note, HDR-based DSB repair was higher in treated primary keratinocytes than immortalized keratinocytes. We observed HDR efficiencies of $\leq$25% in early passage (P1) RDEB223 keratinocytes, resulting in the introduction of the target c.425G>A (WT) SNP in about 21% of NGS-analyzed alleles (Figure 6B). NGS analysis revealed that the main proportion of corrected alleles harbored both SNPs, the c.425G>A (WT) SNP together with the c.426+7C>A SNP, which results in the inactivation of the former PAM site (data not shown). To identify whether the c.426+7C>A SNP introduced at the 5′ site of intron 3 modulates *COL7A1* splicing during mRNA maturation, we analyzed the cDNA/mRNA of treated primary RDEB223 keratinocytes. Real-time (RT)-based PCR amplification of the *COL7A1* target site via flanking exon-junction primers (Table S2) revealed the presence of corrected *COL7A1* transcripts. These were absent in untreated RDEB keratinocytes (Figure S12A). Subsequent Sanger sequencing of PCR subclones revealed correctly spliced *COL7A1* fragments in ~66% of amplicons (Figure S12B). Additionally, the three main transcript variants, already described for homozygous c.425A>G RDEB cells, were detectable and validated by Sanger sequencing (Figure S12B).[48]

Western blot analysis of treated primary RDEB keratinocytes confirmed full-length C7 restoration and its accurate secretion (Figure 6C). Restored C7 expression was visualized in treated cells via co-immunofluorescence staining (Figure 6D) and quantified via flow cytometric analysis, resulting in C7 restoration in over 37% of RNP/ssOligo-treated primary RDEB keratinocytes (Figure S13). From this bulk population, we isolated single-cell clones displaying either absent (clones 1 and 2) or restored C7 expression (clones 3 and 4) (Figure 6E). Ki-67 staining indicated a high proliferative capacity for all analyzed and isolated primary keratinocytes seeded onto feeder layers (Figure 6E). Co-staining of C7 and p63 revealed the presence of p63 within the nuclei of all analyzed cell clones, further supporting this high proliferative capacity (Figure S14).

To confirm the corrective potential of Cas9n RNP and ssOligo, we additionally treated two primary patient keratinocyte cell lines that harbor compound heterozygous mutations (RDEB29 and RDEB30) and two that harbor a homozygous c.425A>G mutation (RDEB223 and RDEB247) within exon 3 of *COL7A1*. T7EI assay indicated similar targeting efficiencies for all treated primary keratinocytes (Figure S15). NGS analysis of treated bulk populations revealed high targeting efficiencies, with indels observed in 68.0% of analyzed reads in RDEB223 and up to 80.5% observed in RDEB29 (Figure S16A). Introduction of the target c.425G>A (WT) SNP ranged from 0.70% (RDEB29) to 19.57% (RDEB223) (Figure S16B). Western blot analyses confirmed C7 expression and restoration in all of our treated and analyzed primary keratinocyte bulk populations, ranging from 9.08% (RDEB30) to 31.46% (RDEB223) compared to normal levels (Figure S16C), confirmed via co-immunofluorescence staining (Figure S16D). Divergences between primary keratinocyte populations regarding *COL7A1* editing and C7 restoration efficiency might be the result of several factors. The mutation distribution (heterozygous or homozygous), proliferative potential, differentiation capacity, and quality of isolated primary RDEB keratinocytes with regard to remaining epidermal stem cells with higher proliferative capacity likely have a significant impact on HDR efficiency. Co-immunofluorescence staining of C7 and Ki-67 clearly indicated distinct proliferative capacity among all four different primary keratinocyte populations. RDEB29 and RDEB30 keratinocytes showed reduced Ki-67 expression and lower amounts of Ki-67-expressing cells compared to RDEB223 and RDEB247 keratinocytes (Figure S16D).

### HDR rates in primary RDEB fibroblasts

In wild-type skin, C7 is expressed in both dermal fibroblasts and basal epidermal keratinocytes. Recently, Supp et al.[49] indicated the need for C7 secretion from both cell types in the formation of structurally normal anchoring fibrils. To confirm the clinical applicability of our approach,

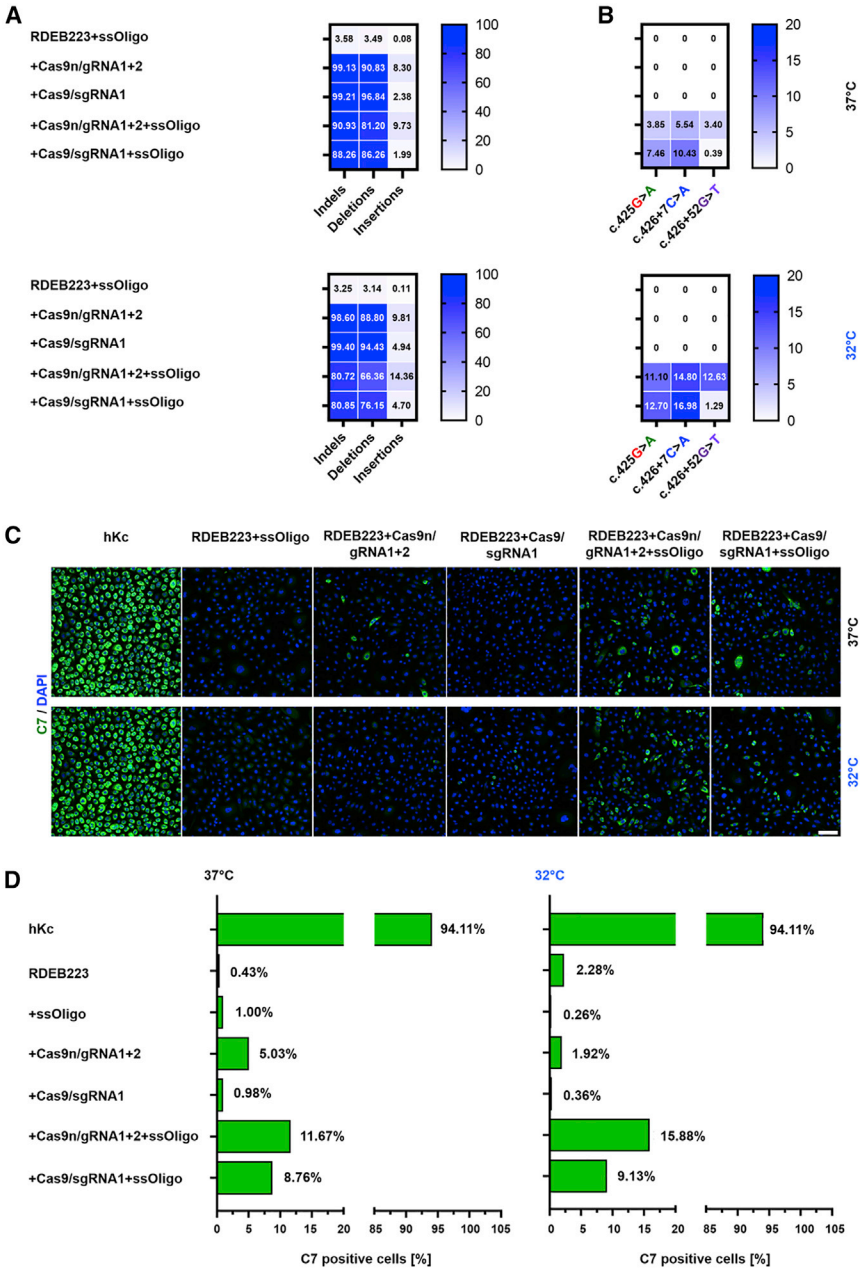


**Figure 5. Cold shock of immortalized RDEB keratinocytes**

(A) NGS analyses of targeting, and (B) HDR efficiencies of Cas9n/gRNA1+2 and Cas9/sgRNA1 RNPs with or without ssOligo-treated bulk populations keratinocytes, cultured at either 37°C or 32°C. (C) Visualization and (D) quantification of restored intracellular C7 via immunofluorescence microscopy and flow cytometry. Scale bar, 100 μm.

### Accurate deposition of C7 within generated 3D SEs

To confirm accurate secretion and deposition of restored C7 within the dermal/epidermal junction, SEs were expanded from partially corrected primary RDEB223 keratinocytes (~37% corrected) and fibroblasts (~12% corrected). Hematoxylin and eosin (H&E) staining of SEs, derived from untreated RDEB keratinocytes and fibroblasts, demonstrated severe blistering within the BMZ. These were reduced in number and size in SEs expanded from RNP/ssOligo-treated patient cells (Figure 8A). Further, immunofluorescence staining of C7 in partially corrected SEs revealed accurate, albeit irregular, deposition of the restored protein within the dermal/epidermal junction (Figure 8B). Notably, C7 was undetectable in SEs composed of either untreated fibroblasts and corrected (~37%) keratinocytes or untreated keratinocytes and corrected (~12%) fibroblasts (data not shown).

## DISCUSSION

Several strategies have been envisioned to ease the burden of RDEB, although a comprehensive cure remains a challenging goal. Throughout this study, we implemented a selection-free HDR-based *COL7A1* editing approach in order to correct a hotspot mutation c.425A>G, causal for this severe blistering skin disease. Gene editing appears to be the most promising advancement in attaining this goal, although current strategies remain far from clinical application. At present, a cutaneous *ex vivo* gene therapy, based on the transplantation of genetically modified keratinocyte stem cells, is the primary focus of EB research. Patient keratinocytes can be easily isolated and expanded on lethally irradiated murine fibroblasts (feeder cells), genetically modified with high efficiency, and transplanted back onto the patient—as successfully demonstrated in recent clinical gene replacement studies.[4,6,7] Although these auspicious studies described the introduction of a full copy of the wild-type gene into patient-derived cells, novel gene-editing approaches hold the distinct advantage of enabling reversion of mutated genes to

we treated patient-matched primary RDEB fibroblasts (RDEB223) with our HDR-based double-nicking strategy. T7EI assay indicated similar RNP targeting efficiencies between treated primary fibroblasts and primary keratinocytes (Figure S11). NGS analysis revealed gene-editing signatures in ~80% of analyzed *COL7A1* alleles (Figure 7A), accompanied by an HDR-mediated gene repair efficiency of over 10% (Figure 7B). Consequently, C7 restoration levels of ~11% and concomitant accurate secretion were detected via western blot analyses (Figure 7C). Quantification of C7 expression via flow cytometric analysis revealed restoration of C7 in ~12% of treated fibroblasts (Figure S17), confirmed and visualized via co-immunofluorescence staining (Figure 7D).

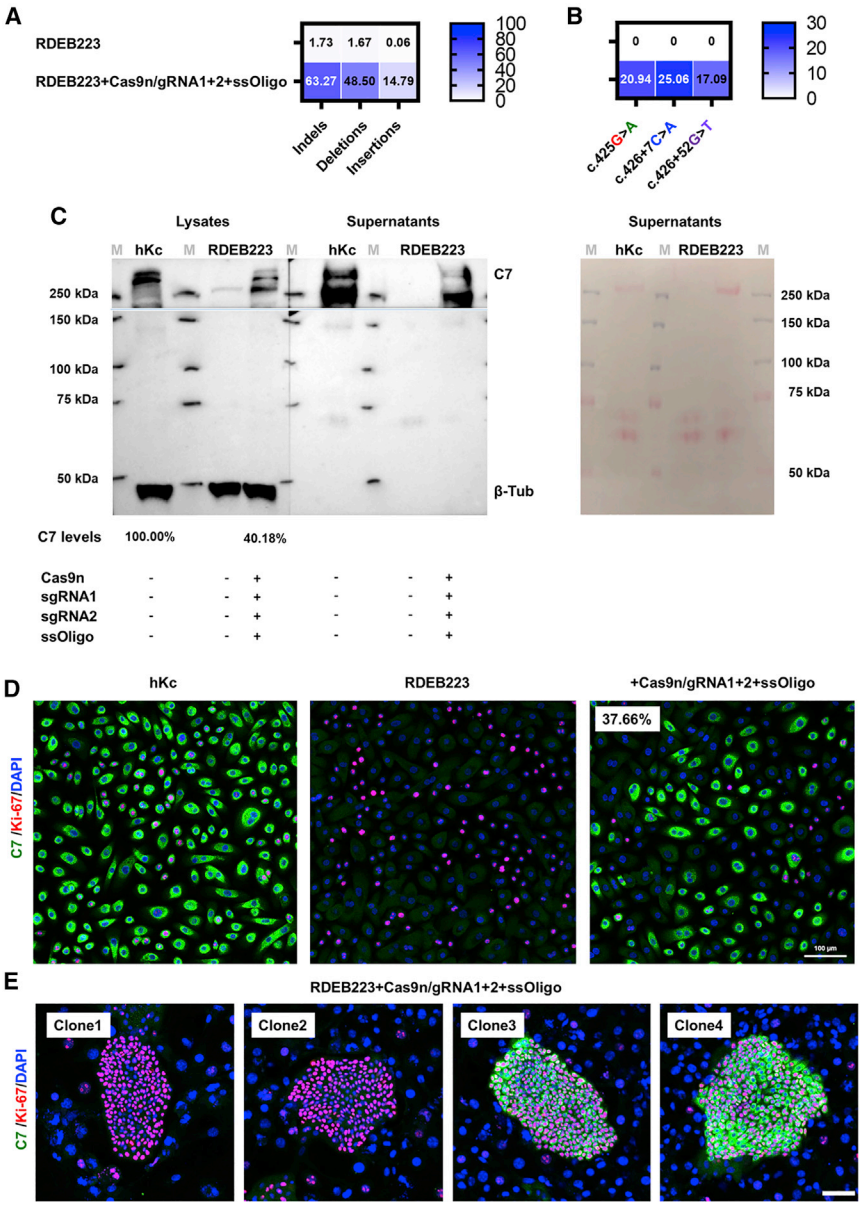


**Figure 6. Analysis of Cas9n/gRNA1+2+ssOligo-treated primary RDEB223 keratinocytes**

Primary keratinocytes were cultured at 32°C for 24 h before and after nucleofection. Keratinocytes were treated with Cas9n/gRNA1+2 RNPs together with ssOligos. (A and B) One week post-treatment, cells were harvested and PCR-amplified genomic on-target regions were NGS analyzed. (A) Heatmap displays the relative amount of indels induced via Cas9 RNPs. (B) Heatmap displays relative amounts of SNPs introduced into the genomic on-target region via HDR. (C) Western blot analyses of cell lysates and supernatants from wild-type, untreated RDEB223 patient-derived keratinocytes and Cas9/gRNA1+2 RNPs together with ssOligo-treated primary RDEB223 patient-derived keratinocytes. Analyses revealed efficient C7 restoration of intracellular protein forms and secretion of C7 into the supernatant in treated primary RDEB keratinocytes. β-tubulin was used as loading control for whole-cell lysates and as purity control for supernatants. Ponceau staining served as loading control for supernatants. Densitometric analysis was performed using the Image Lab 6.0.1 software. C7 levels are shown as % of relative C7 expression normalized to β-tubulin. (D) Co-immunofluorescence staining of C7 (green) and Ki-67 (red) in primary RDEB223 patient and Cas9n/gRNA1+2 RNPs and ssOligo-treated keratinocyte bulk population monolayers confirmed restoration of C7 protein expression. The relative number of C7-expressing cells was estimated via flow cytometric analyses. Scale bar, 100 μm. (E) Co-immunofluorescence staining against C7 (green) and Ki-67 (red) of single-cell clones cultured on feeder layers. Clones 1 and 2 represent clones of primary patient-derived keratinocytes lacking C7 expression after treatment. Clones 3 and 4 represent clones re-expressing C7 after Cas9n/gRNA1+2+ssOligo treatment. Scale bar, 100 μm.

wild-type through the use of DNA-modifying agents such as CRISPR-Cas9. In contrast to highly efficient EJ-based gene-editing strategies, HDR-based approaches currently represent the optimal strategy for achieving perfect, traceless repair in EB, albeit with lower associated efficiencies.[18,20,50] In this study, we aimed to develop an improved HDR-based approach from an efficiency and safety perspective. To this end, we employed an efficient and specific approach that we have previously described.[13] Our previous studies demonstrated that targeting via the D10A nickase variant of the Cas9 from *Streptococcus pyogenes*, which preferably induces SSBs within the DNA, led to the restoration of gene function in EB.[13,27,33,36] Further, we demonstrated that paired nicking resulted in auspicious HDR rates and reduced off-target effects.[13,36] However, the reliance on selection-based protocols and possible HDR donor sequence integrations at off-target sites remained the greatest hurdles for future clinical applications.[13]

In HDR approaches, antibiotic- or fluorescence-based selection cassettes are typically inserted within the donor plasmid to allow for the selection of transfected and/or modified cell clones.[13,15,26,27,30,51] This can lead to remarkable HDR (≤89%) and C7 restoration (≤77%) efficiencies in immortalized RDEB keratinocytes.[13] Additionally, subtle template modifications and strategic template nicking can further improve HDR efficiencies in treated RDEB keratinocytes.[13] Recently, Jacków et al.[30] performed an HDR-based approach in order to achieve a traceless correction of RDEB using induced pluripotent stem cells (iPSCs). Similar to the strategy utilized in our study, they progressed from a plasmid-based system to a protein-based RNP delivery system. They subsequently demonstrated repair of RDEB-causing mutations, following electroporation of RNPs and ssOligos into patient-derived iPSCs. The co-transfection of a GFP-encoding plasmid further

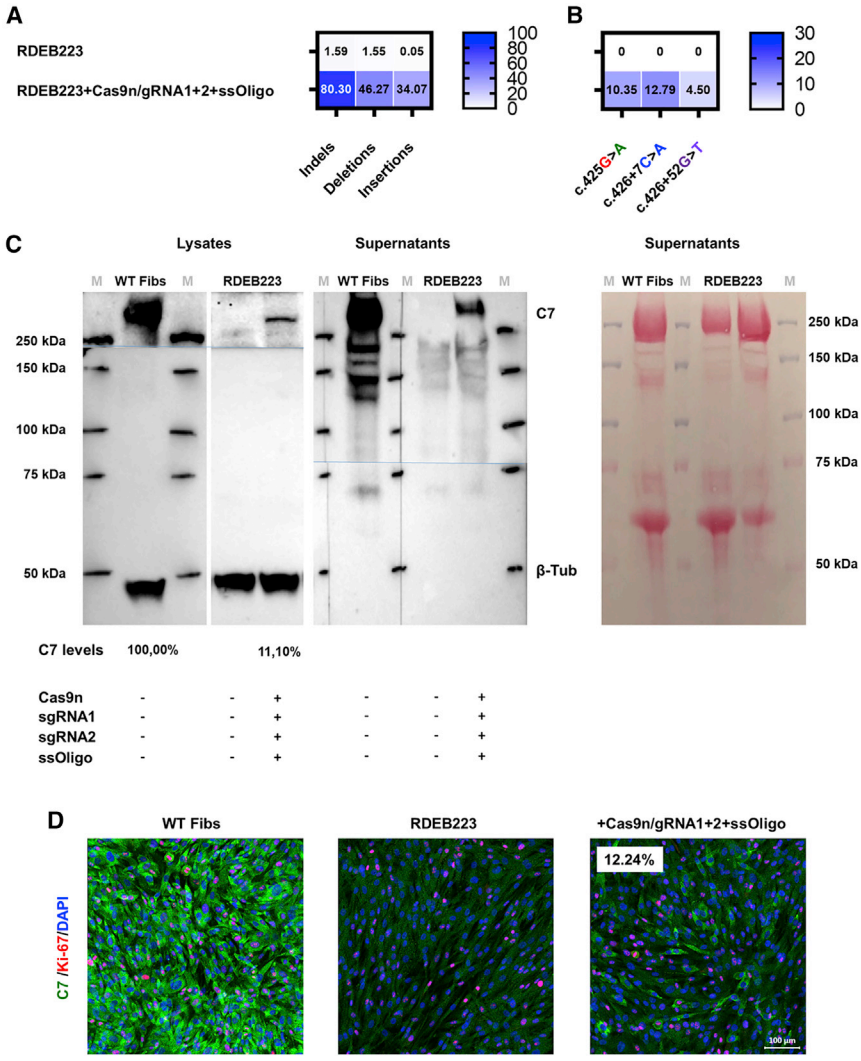


**Figure 7. Analysis of Cas9n/gRNA1+2+ssOligo-treated primary RDEB223 fibroblasts**

Primary fibroblasts were treated with Cas9n/gRNA1+2 RNPs together with ssOligos. (A and B) One week post-treatment, cells were harvested and PCR-amplified genomic on-target regions were analyzed via NGS. (A) Heatmap displays relative indel formation (indels) induced via Cas9 RNPs. (B) Heatmap displays relative SNP introduction into the genomic on-target region via HDR. (C) Western blot analyses of cell lysates and supernatants from wild-type, untreated RDEB223 patient-derived fibroblasts and Cas9/gRNA1+2 RNPs together with ssOligo-treated primary RDEB223 patient-derived fibroblasts. Analyses revealed efficient C7 restoration of intracellular protein forms in treated primary RDEB fibroblasts and secretion of C7 into the supernatant. β-tubulin was used as loading control for whole-cell lysates and as purity control for supernatants. Ponceau staining served as loading control for supernatants. Densitometric analysis was performed using the Image Lab 6.0.1 software. C7 levels are shown as % of relative C7 expression normalized to β-tubulin. (D) Co-immunofluorescence staining of C7 (green) and Ki-67 (red) in primary RDEB223 patient, Cas9n/gRNA1+2 RNPs, and ssOligo-treated fibroblast monolayers confirmed restoration of C7 protein expression. The relative number of C7-expressing cells was estimated via flow cytometric analyses. Scale bar, 100 μm.

enabled fluorescence-activated cell sorting (FACS)-based isolation of transfected, and therefore possibly gene-edited, clones out of the bulk cell population without the requirement of a drug selection cassette. Hence, they achieved an HDR-based gene correction efficiency of $\leq$58%.[30] Recently, Bonafont et al.[52] demonstrated similar *COL7A1* correction efficiencies in primary RDEB keratinocytes following targeting of intron 79 via electroporation of RNPs and adeno-associated virus (AAV)-mediated delivery of single-stranded DNA repair templates. 3D human skin equivalents (HSEs), grafted onto immune-deficient mice, demonstrated accurate deposition of C7 at the BMZ in both studies.[30,52] The inclusion of C7-expressing skin cell types (fibroblasts and keratinocytes) in SEs is likely to be fundamental to create structurally normal C7 anchoring fibrils within the BMZ in order to improve long-term functionality and stability.[30,49]

Due to significant concerns that our initial selection-based strategy might lead to random or targeted partial integrations of the donor template sequence, we followed a similar gene-editing strategy to Jacków et al.[30] and Bonafont et al.,[52] although in our approach, no foreign DNA-reliant selection and no viral transduction were performed.[13] We electroporated Cas9 RNPs together with single- or double-stranded Oligos into patient keratinocytes to correct a prevalent RDEB-associated mutation (c.425A>G) within exon 3 of *COL7A1*. The avoidance of plasmid-based Cas9 expression, selection systems, or viral transduction, and the use of a Cas9 nickase are expected to increase the safety of the approach significantly. However, comparable to our plasmid-based approach, we detected a high RNP-mediated targeting efficiency of ~96% at a previously characterized off-target site in treated RDEB keratinocytes via NGS.[13] Further, the co-treatment of patient cells with single- or double-stranded Oligos led to a remarkable increase in insertion rates at the off-target site, especially when dsOligos were applied. A partial dsOligo sequence (27–30 nt) was dominantly (~10% of insertions) integrated at the RNP targeting site. This phenomenon was only observed when cells were treated with wild-type Cas9/sgRNA1. In addition to the previously sequence-alignment predicted and characterized sgRNA1 off-target site, Abnoba-Seq analysis for *in vitro* prediction of possible off-target sites suggested further off-target sites for both sgRNAs (1 and 2). Subsequent NGS analysis of 12 *in vitro* identified off-target sites (6 for each sgRNA) confirmed minor (0.09%–0.38% of total reads) off-target activity at 5 (3 for sgRNA1 and 2 for sgRNA2) genomic loci, following treatment of patient-derived keratinocytes with wild-type

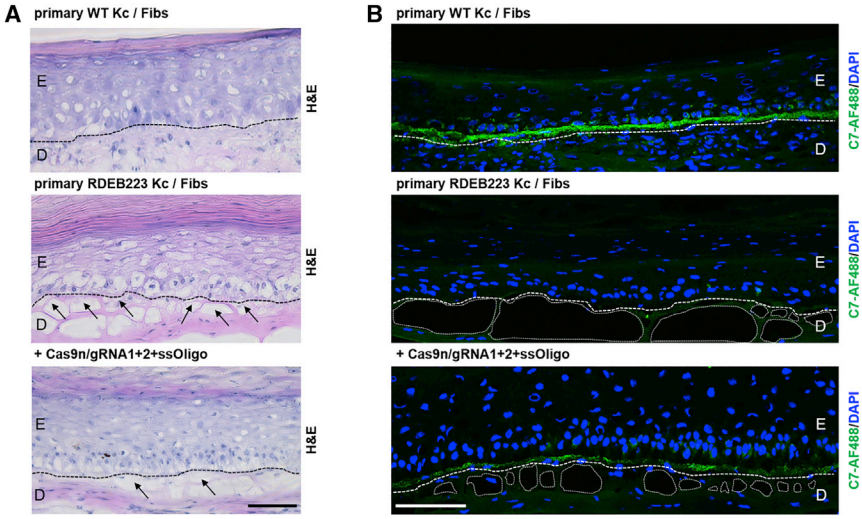


**Figure 8. Localization of type VII collagen in cryosections of engineered 3D skin equivalents (SEs) *in vitro***

(A) Hematoxylin and eosin (H&E) staining of SEs expanded from primary wild-type keratinocytes, untreated primary RDEB keratinocytes and fibroblasts, and RNP-treated primary RDEB keratinocytes and fibroblasts. Dotted line indicates the deviation of the basement membrane zone (BMZ). Scale bar, 100 μm. E, epidermis; D, dermis (black arrows indicate dermal blisters around the BMZ). (B) Immunofluorescence staining of C7 (green) within SEs expanded from the RNP-treated bulk keratinocyte and fibroblast populations revealed partial deposition of restored C7 within the BMZ. SEs derived from wild-type keratinocytes and untreated RDEB keratinocytes served as positive and negative control, respectively. Scale bar, 100 μm. E, epidermis; D, dermis (white dotted line indicate the BMZ; white dotted circles indicate blisters around the epidermal-dermal junction).

Cas9 nuclease. In contrast, no off-target events were detected in nickase-treated RDEB keratinocytes, highlighting the improved safety profile of this targeting strategy.

Computational off-target alignment and *in vitro* identification of possible off-target sites often identifies distinct off-targets. Although the skin theoretically enables careful monitoring of modified tissues in patients, grafted sites must be monitored long term in order to screen for the development of skin cancer that may not be immediately observed. To reduce these long-term risks, screening via combined off-target prediction strategies is highly recommended prior to the transplantation of *ex vivo*-corrected skin sheets.

Genome-wide, unbiased identification of DSBs enabled by sequencing (GUIDE-seq) and circularization for *in vitro* reporting of cleavage effects by sequencing (CIRCLE-seq) comprise two sensitive sequencing-efficient *in vitro* off-target screening strategies to identify CRISPR-Cas9 genome-wide off-target events.[53,54] GUIDE-seq relies on the capture of double-stranded oligodeoxynucleotides into DNA breaks for identification of sites not detected by current computational methods or chromatin immunoprecipitation sequencing (ChIP-seq).[53] CIRCLE-seq is a sensitive circularization-dependent strategy for *in vitro* reporting of cleavage sites, postulated to outperform existing cell-based or biochemical approaches for identifying CRISPR-Cas9 genome-wide off-target mutations. Furthermore, CIRCLE-seq can identify off-target mutations associated with cell-type-specific SNPs, which could be important for generating personalized specificity profiles for future clinical applications.[54]

Linear Amplification Mediated (LAM)-PCR-based approaches and the recently published chromosomal aberrations analysis by single targeted linker-mediated PCR sequencing (CAST-seq) method for the detection of chromosomal translocations are promising tools to further assess the risk of genotoxicity of genome editing on a chromosomal level.[55,56] CAST-seq is a sensitive assay suitable for the identification and quantification of unintended chromosomal rearrangements, representing a valuable approach to enable thorough risk assessment before clinical application of gene-edited cell products.[56]

However, above all considerations, improved repair efficiencies are pivotal for advancing experimental gene therapies into clinical settings. Concerning RDEB, prior studies estimate a correction efficiency of 35% to be sufficient for a complete phenotypic reversion *in vitro* and *in vivo*.[57,58] To combine an improved safety profile with increased HDR and correction rates, we utilized paired Cas9 nickases together with an ssOligo repair template resulting in HDR-mediated correction efficiencies of >20% in primary RDEB keratinocytes and >10% in primary fibroblasts at the genomic level and >37% and >12% at a cellular level, respectively. Here, pre-incubation of cells at 32°C had a positive impact on the overall HDR efficiency. To our knowledge, this is the highest HDR-based gene-editing efficiency achieved for EB without viral transduction and selection for transfected and/or gene-edited cells. Notably, H&E and C7 immunofluorescence staining of SEs, derived from bulk-treated, corrected primary RDEB keratinocytes and fibroblasts, indicated an improved phenotype regarding blister formation and C7 deposition within the BMZ. Although the treatment did not result in homogeneous C7 expression along the dermal/epidermal junction, skin stability is predicted to be improved. However, this requires investigation via intended transplantation studies applied in recent gene-editing-based approaches undertaken within our group.[27,59] Animal studies would enable further assessment of skin functionality and stability, in addition to the long-term viability and functionality of edited cells in an environment in which they would compete with unmodified cells. Pre-clinical testing in animal models in conjunction with extensive off-target screening on an allelic and chromosomal level are critical before clinical application of gene-editing therapies.

Good Manufacturing Practice (GMP)-grade Cas9 proteins, sgRNAs, and commercially available electroporators for large-scale cell

treatment will pave the way for efficient clinical *ex vivo* gene-editing applications. Delivery of CRISPR-Cas9 into target cells via RNP electroporation has been shown to result in high on-target efficiencies accompanied by low off-target activities.[18,20,52] To our knowledge, there is no other alternative *in vitro* delivery method as efficient as electroporation. Despite this, future investigations into the clinical applicability of this approach must also address the high RNP-induced on-target indel frequencies accompanying the desired perfect repair outcome. This could likely be mitigated in part by alternative precise genome editing technologies, such as base editing or prime editing, which also rely on targeting via Cas9 nickases.[21,23]

However, currently, the combined delivery of paired nicking RNPs with ssOligos represents an advanced HDR-based gene correction strategy for RDEB, enabling perfect repair of *COL7A1* in terms of efficiency, safety, and precision.

## MATERIALS AND METHODS

### Cell culture, transfection, and clonal expansion

Primary RDEB keratinocytes (RDEB29, RDEB30, RDEB223, RDEB247) and primary fibroblasts (RDEB223) were isolated from skin biopsies from patients carrying the following *COL7A1* mutations: RDEB29: c.425A>G/c.520G>A; RDEB30: c.425A>G/c.520G>A; RDEB223: c.425A>G/c.425A>G; RDEB247: c.425A>G/c.425A>G. Primary RDEB keratinocytes were immortalized through transduction of the human papilloma virus proteins E6 and E7.[60] Prior to cell isolation, patients' signed informed consents were obtained. All cell lines were maintained at 37°C and 5% carbon dioxide in a humidified incubator. One day before electroporation, antibiotic-free media was added to the cells. For cold shock experiments, cells were shifted to 32°C 1 day before treatment and further incubated on 32°C for another 24 h after electroporation, before switching back to 37°C. RNP electroporations were performed using the Neon transfection system (Thermo Fisher Scientific, Waltham, MA, USA) with the following settings: 1,400 volts, 20 ms, 2 pulses. RNPs were complexed in a 4:1 ratio using 3 μg Cas9/Cas9n together with 750 ng sgRNA. $3 \times 10^5$ cells were used for each single treatment. Wild-type keratinocytes, untransfected RDEB keratinocytes, wild-type fibroblasts, and untransfected RDEB fibroblasts served as controls. For clonal expansion, RNP-treated primary cells were isolated ~7 days after transfection and seeded at low density onto 3T3-J2 mouse fibroblast feeder cells ($5–8 \times 10^3$ cells/$cm^2$), which were initially growth arrested with 4 μg/mL mitomycin C (Roche, Basel, Switzerland) for 2 h at 37°C.[18]

### Flow cytometric analysis

Initially, cells were fixed and permeabilized with Fix/Perm Solution (Thermo Fisher Scientific) for 45 min. After two washing steps in Perm Buffer (Thermo Fisher Scientific) and blocking in 10% sheep serum (Sigma-Aldrich, St. Louis, MO, USA) for 10 min, a polyclonal C7 antibody was added as primary antibody, diluted 1:1,000 in PBS.[61] Cells were incubated for 30 min at 4°C, washed with Perm Buffer, and incubated with the secondary antibody (goat anti-rabbit FITS) (BD Biosciences, San Jose, CA, USA) for an additional 30 min, in a dilution of 1:25 in PBS in the dark at 4°C. Cells were maintained in PBS and analyzed using either the Gallios Flow Cytometer (Beckman Coulter, Krefeld, Germany) or the LSR-Fortessa (BD Biosciences). Data analysis was performed using the Kaluza software.

### Immunofluorescence staining of monolayers and single-cell clones

Prior to immunofluorescence staining, $1 \times 10^5$ keratinocytes were seeded into μ-Slide 8 well chamber slides (ibidi, Gräfelfing, Germany) and grown to 70%–100% confluence. For single-cell clone analyses, growth-arrested 3T3-J2 mouse fibroblast feeder cells were seeded ($6 \times 10^4$ feeder cells/well) into μ-Slide 8-well chamber slides. RNP-treated primary cells (~7 days post transfection) were seeded onto the feeder layer at low density (~$1 \times 10^3$ cells/well). Single-cell clones were expanded for at least 1 week prior to fixing with 4% formaldehyde solution (SAV Liquid Production, Flintsbach am Inn, Germany) for 10 min at RT. The subsequent permeabilization and co-staining of the cells was performed in a single step. A human-specific rabbit anti-C7 antibody was used in a 1:5,000 dilution together with a mouse anti-Ki-67 (8D5) antibody (Cell Signaling Technology Europe, Leiden, the Netherlands) in a 1:1,000 dilution or a mouse anti-p63 (4A4) antibody (Abcam, Cambridge, UK) in a 1:500 dilution.[61] Dilutions were performed in 0.3% Triton-X blocking reagent (1:10) and Tris-buffered saline with 0.2% Tween (TBS-T). Incubation with primary antibody lasted for 2 h at RT. After two washing steps with PBS, cells were co-stained with Alexa Fluor 488 goat anti-rabbit IgG (H+L) and Alexa Fluor 594 goat anti-mouse IgG (H+L) secondary antibodies (Thermo Fisher Scientific) (1:300 in TBS-T) for 1 h at RT. Cell nuclei staining via DAPI (4′,6-diamidin-2-phenylindol) (1:4,000 in TBS-T) was performed for 10 min at RT. Stained cells were analyzed using an inverted microscope system, including the laser scanning confocal microscope Zeiss LSM 700 and the Axio Observer Z1 (Carl Zeiss, Oberkochen, Germany).

### Generation of SEs and immunofluorescence staining

SE generation and immunofluorescence staining were performed as recently described.[18] SEs were generated using human fibrin as scaffold for primary wild-type, primary RDEB223, and treated primary RDEB223 human fibroblasts in 12-well plates. Primary wild-type keratinocytes, primary RDEB223 keratinocytes, and RNP/ssOligo-treated primary RDEB keratinocytes ($3 \times 10^4$ cells per well) were seeded onto the matrix, grown to confluence, and raised at the air-liquid interface for 7 days to favor stratification and differentiation into an epithelium.

### T7EI assay

Sequence mismatches, resulting from Cas9/sgRNA-mediated DSBs and subsequent NHEJ at the desired genomic loci in RNP-treated RDEB keratinocytes and fibroblasts, were evaluated via T7EI assay (New England Biolabs, Frankfurt, Germany). Initially, the *COL7A1* on-target site and the off-target site 7 (formerly described as OT9) were PCR amplified using specific primer pairs, flanking the respective cutting sites.[13] T7EI digest of the resulting PCR fragment was performed according to the manufacturer's protocol (see Table S2 for primer sequences).

### Splicing analysis

Total RNA was isolated from cultured primary wild-type, RDEB223, and treated RDEB223 keratinocytes using an innu-PREP RNA Mini Kit (Analytik Jena, Jena, Germany). cDNA was synthesized from 1 μg of total RNA, using LunaScript RT SuperMix Kit (New England Biolabs, Frankfurt am Main, Germany). For amplification of the transcripts, *COL7A1* exon1-exon2 forward and exon4-exon5 reverse primers were used. For subcloning of the PCR product, the StrataClone PCR Cloning Kit (Aligent Technologies, Santa Clara, CA, USA) was used according to the manufacturer's protocol. Single clones and resulting PCR products were Sanger sequenced and subsequently analyzed via CRISPR-ID.[62]

### Protein isolation and western blot analysis

For cell lysis, cell pellets were dissolved in radioimmunoprecipitation assay buffer (Santa Cruz Biotechnology, Heidelberg, Germany). Whole-cell lysates were subsequently centrifuged at full speed at 4°C for 20 min and supernatant was frozen at −20°C. Protein precipitation from cell culture supernatants was performed as recently described.[13] Following denaturation of protein samples for 5 min at 95°C in 4× loading buffer (0.25 M Tris-hydrochloride, 8% SDS, 30% glycerol, 0.02% bromophenol blue, 0.3 M b-mercaptoethanol [pH: 6.8]), lysates were loaded onto 8% Bis-Tris Plus gels and western blot analysis was performed as recently described.[13,18] Loaded protein was estimated via Ponceau red (Sigma-Aldrich) staining after electroblotting. Following blocking of the nitrocellulose membrane using the blocking reagent from Roche Diagnostics (Roche Diagnostics, Mannheim, Germany) in a dilution of 1:10 in TBS-T for 1 h at RT, an N-terminal anti-C7 antibody (clone LH7.2) was added in a dilution of 1:5,000 in TBS-T.[61] The membrane was subsequently incubated overnight at 4°C. For loading control staining, a polyclonal β-tubulin antibody (ab6064) (Abcam, Cambridge, UK) was used in a dilution of 1:2,000 in TBS-T and blocking reagent. Secondary antibodies, the HRP Envision+-labeled anti-rabbit and the HRP Envision+-labeled anti-mouse antibody (Dako, Santa Clara, CA, USA), were 1:300 diluted in TBS-T. The nitrocellulose membrane was subsequently incubated for 1 h at RT. Visualization of protein bands was performed through the Immobilon Western Chemiluminescent HRP Substrate (Merck, Darmstadt, Germany) and the ChemiDoc XRS Imager (Bio-Rad, Hercules, CA, USA). One of three representative western blot analyses for primary RDEB keratinocytes and fibroblasts is shown in Figures 6, 7, and S16.

### NGS: On-target region

Kapa Hifi Hot Start Ready Mix (Roche, Basel, Switzerland) was used for PCR amplification of the *COL7A1* on-target region of treated and untreated keratinocytes according to the manufacturer's protocol. Primers were tagged with adapters for Illumina Nextera indexes (see Table S3 for primer sequences). PCR amplicons were subsequently purified with Kapa Pure Beads (Roche; Basel, Switzerland) according to the manufacturer's protocol. In order to remove primer dimers, fragments below 200 bp were excluded by this purification step. Index PCRs were performed with the Nextera XT Index Kit v.2 Set A (Illumina, San Diego, CA, USA) and Kapa Hifi Hot Start Ready Mix. PCRs were again purified with Kapa Pure Beads, excluding fragments below 200 bp. Purified amplicons were quantified using the Qubit 2 Fluorometer and the Qubit dsDNA HS Assay Kit (Thermo Fisher Scientific). Samples were subsequently pooled and sent for Illumina MiSeq Sequencing at the Vienna BioCenter Next-Generation Sequencing Facility (Vienna BioCenter Core Facilities, Vienna, Austria). Analysis of genome-editing outcomes from deep-sequencing data was either performed via the CRISPResso2 online platform or the CRISPR RGEN Tools Cas-Analyzer.[63,64]

### Unbiased off-target analysis

Abnoba-Seq is a genome-wide, unbiased, and highly sensitive method to profile the off-target activity of CRISPR-Cas nuclease *in vitro*.[39] Briefly, genomic DNA of primary human keratinocytes was isolated, fragmented, end-blocked, and cleaved *in vitro* with CRISPR-Cas9 RNPs loaded with the respective sgRNAs. Cleaved DNA ends were tagged with biotinylated adaptors. Upon streptavidin-based enrichment, the DNA fragments were amplified by PCR and subjected to NGS. Aligning the sequence reads to a human reference genome revealed off-target sites.

### Institutional approval of experiments

All performed experiments were executed under biosafety level 2 conditions. The work, including the work with wild-type and patient cells used in the study, was biosafety level 2 approved by the local authorities (Federal Ministry of Labor, Social Affairs, Health, and Consumer Protection). In this study, we used human keratinocytes and fibroblasts obtained from skin biopsies or hair follicles donated following informed consent of the healthy volunteer or the patient.

### Data availability statement

Datasets related to this article can be found at: https://dx.doi.org/10.17632/ttmgw6rjct.2.

## SUPPLEMENTAL INFORMATION

Supplemental information can be found online at https://doi.org/10.1016/j.omtn.2021.05.015.

## ACKNOWLEDGMENTS

The authors thank Univ.-Prof. Dr. Eva Rohde and Karin Roider, MSc of the Spinal Cord Injury and Tissue Regeneration Center Salzburg (SCI-TReCS) for providing their Core Facility for Microscopy. Further, we thank Prof. Dr. Andreas Traweger from the Institute of Tendon and Bone Regeneration (SCI-TReCS) for providing the cryotome. Thanks to Dr. Alexander Nyström from the Department of Dermatology, Medical Center – University of Freiburg, Germany, who kindly provided the type VII collagen antibody. Sequencing was performed at the VBCF NGS Unit (https://www.viennabiocenter.org/facilities). This work was supported by DEBRA Austria and the German Federal Ministry of Education and Research.

## AUTHOR CONTRIBUTIONS

U.K. conceived and supervised this study. T.K. and U.K. were involved in study design. T.K., J.B., B.L., S.A.H., A.H., K.M.,

H.M.B., J.I., A.K., and S.H. conducted the experiments and interpreted all results. D.S., T.C., J.W.B., and U.K. provided funding for this study. T.K., O.P.M., and U.K. wrote the manuscript. T.K., O.P.M., D.S., T.C., J.W.B., and U.K were substantially involved in paper editing. All authors critically reviewed the manuscript.

## DECLARATION OF INTERESTS

T.C. and S.A.H. have filed a patent application for Abnoba-Seq. T.C. has sponsored research collaborations with Cellectis and Miltenyi. All other authors declare no competing interests.

## REFERENCES


1. Has, C., Bauer, J.W., Bodemer, C., Bolling, M.C., Bruckner-Tuderman, L., Diem, A., Fine, J.D., Heagerty, A., Hovnanian, A., Marinkovich, M.P., et al. (2020). Consensus reclassification of inherited epidermolysis bullosa and other disorders with skin fragility. Br. J. Dermatol. *183*, 614–627.
2. Fine, J.D., Bruckner-Tuderman, L., Eady, R.A.J., Bauer, E.A., Bauer, J.W., Has, C., Heagerty, A., Hintner, H., Hovnanian, A., Jonkman, M.F., et al. (2014). Inherited epidermolysis bullosa: updated recommendations on diagnosis and classification. J. Am. Acad. Dermatol. *70*, 1103–1126.
3. Montaudié, H., Chiaverini, C., Sbidian, E., Charlesworth, A., and Lacour, J.P. (2016). Inherited epidermolysis bullosa and squamous cell carcinoma: a systematic review of 117 cases. Orphanet J. Rare Dis. *11*, 117.
4. Hirsch, T., Rothoeft, T., Teig, N., Bauer, J.W., Pellegrini, G., De Rosa, L., Scaglione, D., Reichelt, J., Klausegger, A., Kneisz, D., et al. (2017). Regeneration of the entire human epidermis using transgenic stem cells. Nature *551*, 327–332.
5. March, O.P., Kocher, T., and Koller, U. (2020). Context-Dependent Strategies for Enhanced Genome Editing of Genodermatoses. Cells *9*, 112.
6. Mavilio, F., Pellegrini, G., Ferrari, S., Di Nunzio, F., Di Iorio, E., Recchia, A., Maruggi, G., Ferrari, G., Provasi, E., Bonini, C., et al. (2006). Correction of junctional epidermolysis bullosa by transplantation of genetically modified epidermal stem cells. Nat. Med. *12*, 1397–1402.
7. Bauer, J.W., Koller, J., Murauer, E.M., De Rosa, L., Enzo, E., Carulli, S., Bondanza, S., Recchia, A., Muss, W., Diem, A., et al. (2017). Closure of a Large Chronic Wound through Transplantation of Gene-Corrected Epidermal Stem Cells. J. Invest. Dermatol. *137*, 778–781.
8. Siprashvili, Z., Nguyen, N.T., Gorell, E.S., Loutit, K., Khuu, P., Furukawa, L.K., Lorenz, H.P., Leung, T.H., Keene, D.R., Rieger, K.E., et al. (2016). Safety and Wound Outcomes Following Genetically Corrected Autologous Epidermal Grafts in Patients With Recessive Dystrophic Epidermolysis Bullosa. JAMA *316*, 1808–1817.
9. Titeux, M., Pendaries, V., Zanta-Boussif, M.A., Décha, A., Pironon, N., Tonasso, L., Mejia, J.E., Brice, A., Danos, O., and Hovnanian, A. (2010). SIN retroviral vectors expressing COL7A1 under human promoters for ex vivo gene therapy of recessive dystrophic epidermolysis bullosa. Mol. Ther. *18*, 1509–1518.
10. Montini, E., Cesana, D., Schmidt, M., Sanvito, F., Bartholomae, C.C., Ranzani, M., Benedicenti, F., Sergi, L.S., Ambrosi, A., Ponzoni, M., et al. (2009). The genotoxic potential of retroviral vectors is strongly modulated by vector design and integration site selection in a mouse model of HSC gene therapy. J. Clin. Invest. *119*, 964–975.
11. Sfeir, A., and Symington, L.S. (2015). Microhomology-Mediated End Joining: A Back-up Survival Mechanism or Dedicated Pathway? Trends Biochem. Sci. *40*, 701–714.
12. Danner, E., Bashir, S., Yumlu, S., Wurst, W., Wefers, B., and Kühn, R. (2017). Control of gene editing by manipulation of DNA repair mechanisms. Mamm. Genome *28*, 262–274.
13. Kocher, T., Wagner, R.N., Klausegger, A., Guttmann-Gruber, C., Hainzl, S., Bauer, J.W., Reichelt, J., and Koller, U. (2019). Improved Double-Nicking Strategies for COL7A1-Editing by Homologous Recombination. Mol. Ther. Nucleic Acids *18*, 496–507.
14. Shinkuma, S., Guo, Z., and Christiano, A.M. (2016). Site-specific genome editing for correction of induced pluripotent stem cells derived from dominant dystrophic epidermolysis bullosa. Proc. Natl. Acad. Sci. USA *113*, 5676–5681.
15. Chamorro, C., Mencía, A., Almarza, D., Duarte, B., Büning, H., Sallach, J., Hausser, I., Del Río, M., Larcher, F., and Murillas, R. (2016). Gene Editing for the Efficient Correction of a Recurrent COL7A1 Mutation in Recessive Dystrophic Epidermolysis Bullosa Keratinocytes. Mol. Ther. Nucleic Acids *5*, e307.
16. Mencía, Á., Chamorro, C., Bonafont, J., Duarte, B., Holguin, A., Illera, N., Llames, S.G., Escámez, M.J., Hausser, I., Del Río, M., et al. (2018). Deletion of a Pathogenic Mutation-Containing Exon of COL7A1 Allows Clonal Gene Editing Correction of RDEB Patient Epidermal Stem Cells. Mol. Ther. Nucleic Acids *11*, 68–78.
17. Takashima, S., Shinkuma, S., Fujita, Y., Nomura, T., Ujiie, H., Natsuga, K., Iwata, H., Nakamura, H., Vorobyev, A., Abe, R., and Shimizu, H. (2019). Efficient Gene Reframing Therapy for Recessive Dystrophic Epidermolysis Bullosa with CRISPR/Cas9. J. Invest. Dermatol *139*, 1711–1721.e4.
18. Kocher, T., March, O.P., Bischof, J., Liemberger, B., Hainzl, S., Klausegger, A., Hoog, A., Strunk, D., Bauer, J.W., and Koller, U. (2020). Predictable CRISPR/Cas9-Mediated COL7A1 Reframing for Dystrophic Epidermolysis Bullosa. J. Invest. Dermatol. *140*, 1985–1993.e5.
19. Wu, W., Lu, Z., Li, F., Wang, W., Qian, N., Duan, J., Zhang, Y., Wang, F., and Chen, T. (2017). Efficient in vivo gene editing using ribonucleoproteins in skin stem cells of recessive dystrophic epidermolysis bullosa mouse model. Proc. Natl. Acad. Sci. USA *114*, 1660–1665.
20. Bonafont, J., Mencía, Á., García, M., Torres, R., Rodríguez, S., Carretero, M., Chacón-Solano, E., Modamio-Høybjør, S., Marinas, L., León, C., et al. (2019). Clinically Relevant Correction of Recessive Dystrophic Epidermolysis Bullosa by Dual sgRNA CRISPR/Cas9-Mediated Gene Editing. Mol. Ther. *27*, 986–998.
21. Komor, A.C., Kim, Y.B., Packer, M.S., Zuris, J.A., and Liu, D.R. (2016). Programmable editing of a target base in genomic DNA without double-stranded DNA cleavage. Nature *533*, 420–424.
22. Osborn, M.J., Newby, G.A., McElroy, A.N., Knipping, F., Nielsen, S.C., Riddle, M.J., Xia, L., Chen, W., Eide, C.R., Webber, B.R., et al. (2020). Base editor correction of COL7A1 in recessive dystrophic epidermolysis bullosa patient-derived fibroblasts and iPSCs. J. Invest. Dermatol. *140*, 338–347.e5.
23. Anzalone, A.V., Randolph, P.B., Davis, J.R., Sousa, A.A., Koblan, L.W., Levy, J.M., Chen, P.J., Wilson, C., Newby, G.A., Raguram, A., and Liu, D.R. (2019). Search-and-replace genome editing without double-strand breaks or donor DNA. Nature *576*, 149–157.
24. Osborn, M.J., Starker, C.G., McElroy, A.N., Webber, B.R., Riddle, M.J., Xia, L., DeFeo, A.P., Gabriel, R., Schmidt, M., von Kalle, C., et al. (2013). TALEN-based gene correction for epidermolysis bullosa. Mol. Ther. *21*, 1151–1159.
25. Sebastiano, V., Zhen, H.H., Haddad, B., Bashkirova, E., Melo, S.P., Wang, P., Leung, T.L., Siprashvili, Z., Tichy, A., Li, J., et al. (2014). Human COL7A1-corrected induced pluripotent stem cells for the treatment of recessive dystrophic epidermolysis bullosa. Sci. Transl. Med. *6*, 264ra163.
26. Webber, B.R., Osborn, M.J., McElroy, A.N., Twaroski, K., Lonetree, C.L., DeFeo, A.P., Xia, L., Eide, C., Lees, C.J., McElmurry, R.T., et al. (2016). CRISPR/Cas9-based genetic correction for recessive dystrophic epidermolysis bullosa. NPJ Regen. Med. *1*, 15014.
27. Hainzl, S., Peking, P., Kocher, T., Murauer, E.M., Larcher, F., Del Rio, M., Duarte, B., Steiner, M., Klausegger, A., Bauer, J.W., et al. (2017). COL7A1 Editing via CRISPR/Cas9 in Recessive Dystrophic Epidermolysis Bullosa. Mol. Ther. *25*, 2573–2584.
28. Izmiryan, A., Danos, O., and Hovnanian, A. (2016). Meganuclease-Mediated COL7A1 Gene Correction for Recessive Dystrophic Epidermolysis Bullosa. J. Invest. Dermatol. *136*, 872–875.
29. Izmiryan, A., Ganier, C., Bovolenta, M., Schmitt, A., Mavilio, F., and Hovnanian, A. (2018). Ex Vivo COL7A1 Correction for Recessive Dystrophic Epidermolysis Bullosa Using CRISPR/Cas9 and Homology-Directed Repair. Mol. Ther. Nucleic Acids *12*, 554–567.
30. Jacków, J., Guo, Z., Hansen, C., Abaci, H.E., Doucet, Y.S., Shin, J.U., Hayashi, R., DeLorenzo, D., Kabata, Y., Shinkuma, S., et al. (2019). CRISPR/Cas9-based targeted genome editing for correction of recessive dystrophic epidermolysis bullosa using iPS cells. Proc. Natl. Acad. Sci. USA *116*, 26846–26852.
31. Porteus, M.H. (2019). A New Class of Medicines through DNA Editing. N. Engl. J. Med. *380*, 947–959.
32. Hendel, A., Bak, R.O., Clark, J.T., Kennedy, A.B., Ryan, D.E., Roy, S., Steinfeld, I., Lunstad, B.D., Kaiser, R.J., Wilkens, A.B., et al. (2015). Chemically modified guide

RNAs enhance CRISPR-Cas genome editing in human primary cells. Nat. Biotechnol. *33*, 985–989.

33. Jinek, M., Chylinski, K., Fonfara, I., Hauer, M., Doudna, J.A., and Charpentier, E. (2012). A programmable dual-RNA-guided DNA endonuclease in adaptive bacterial immunity. Science *337*, 816–821.
34. Mali, P., Yang, L., Esvelt, K.M., Aach, J., Guell, M., DiCarlo, J.E., Norville, J.E., and Church, G.M. (2013). RNA-guided human genome engineering via Cas9. Science *339*, 823–826.
35. Ran, F.A., Hsu, P.D., Lin, C.Y., Gootenberg, J.S., Konermann, S., Trevino, A.E., Scott, D.A., Inoue, A., Matoba, S., Zhang, Y., and Zhang, F. (2013). Double nicking by RNA-guided CRISPR Cas9 for enhanced genome editing specificity. Cell *154*, 1380–1389.
36. Kocher, T., Peking, P., Klausegger, A., Murauer, E.M., Hofbauer, J.P., Wally, V., Lettner, T., Hainzl, S., Ablinger, M., Bauer, J.W., et al. (2017). Cut and Paste: Efficient Homology-Directed Repair of a Dominant Negative KRT14 Mutation via CRISPR/Cas9 Nickases. Mol. Ther. *25*, 2585–2598.
37. Guo, Q., Mintier, G., Ma-Edmonds, M., Storton, D., Wang, X., Xiao, X., Kienzle, B., Zhao, D., and Feder, J.N. (2018). 'Cold shock' increases the frequency of homology directed repair gene editing in induced pluripotent stem cells. Sci. Rep. *8*, 2080.
38. Liang, X., Potter, J., Kumar, S., Ravinder, N., and Chesnut, J.D. (2017). Enhanced CRISPR/Cas9-mediated precise genome editing by improved design and delivery of gRNA, Cas9 nuclease, and donor DNA. J. Biotechnol. *241*, 136–146.
39. Haas, S.A. (2019). Tracing the specificity of CRISPR-Cas nucleases in clinically relevant human cells. Institute for Transfusion Medicine and Gene Therapy, Ph.D. Thesis (University of Freiburg, Germany).
40. Maruyama, T., Dougan, S.K., Truttmann, M.C., Bilate, A.M., Ingram, J.R., and Ploegh, H.L. (2015). Increasing the efficiency of precise genome editing with CRISPR-Cas9 by inhibition of nonhomologous end joining. Nat. Biotechnol. *33*, 538–542.
41. Ma, X., Chen, X., Jin, Y., Ge, W., Wang, W., Kong, L., Ji, J., Guo, X., Huang, J., Feng, X.H., et al. (2018). Small molecules promote CRISPR-Cpf1-mediated genome editing in human pluripotent stem cells. Nat. Commun. *9*, 1303.
42. Riesenberg, S., and Maricic, T. (2018). Targeting repair pathways with small molecules increases precise genome editing in pluripotent stem cells. Nat. Commun. *9*, 2164.
43. Savic, N., Ringnalda, F.C., Lindsay, H., Berk, C., Bargsten, K., Li, Y., Neri, D., Robinson, M.D., Ciaudo, C., Hall, J., et al. (2018). Covalent linkage of the DNA repair template to the CRISPR-Cas9 nuclease enhances homology-directed repair. eLife *7*, e33761.
44. Carlson-Stevermer, J., Abdeen, A.A., Kohlenberg, L., Goedland, M., Molugu, K., Lou, M., and Saha, K. (2017). Assembly of CRISPR ribonucleoproteins with biotinylated oligonucleotides via an RNA aptamer for precise gene editing. Nat. Commun. *8*, 1711.
45. Skarnes, W.C., Pellegrino, E., and McDonough, J.A. (2019). Improving homology-directed repair efficiency in human stem cells. Methods *164-165*, 18–28.
46. Lin, S., Staahl, B.T., Alla, R.K., and Doudna, J.A. (2014). Enhanced homology-directed human genome engineering by controlled timing of CRISPR/Cas9 delivery. eLife *3*, e04766.
47. Gu, B., Posfai, E., and Rossant, J. (2018). Efficient generation of targeted large insertions by microinjection into two-cell-stage mouse embryos. Nat. Biotechnol. *36*, 632–637.
48. Gardella, R., Belletti, L., Zoppi, N., Marini, D., Barlati, S., and Colombi, M. (1996). Identification of two splicing mutations in the collagen type VII gene (COL7A1) of a patient affected by the localisata variant of recessive dystrophic epidermolysis bullosa. Am. J. Hum. Genet. *59*, 292–300.
49. Supp, D.M., Hahn, J.M., Combs, K.A., McFarland, K.L., Schwentker, A., Boissy, R.E., Boyce, S.T., Powell, H.M., and Lucky, A.W. (2019). Collagen VII Expression Is Required in Both Keratinocytes and Fibroblasts for Anchoring Fibril Formation in Bilayer Engineered Skin Substitutes. Cell Transplant. *28*, 1242–1256.
50. Aushev, M., Koller, U., Mussolino, C., Cathomen, T., and Reichelt, J. (2017). Traceless Targeting and Isolation of Gene-Edited Immortalized Keratinocytes from Epidermolysis Bullosa Simplex Patients. Mol. Ther. Methods Clin. Dev *6*, 112–123.
51. Itoh, M., Kawagoe, S., Tamai, K., Nakagawa, H., Asahina, A., and Okano, H.J. (2020). Footprint-free gene mutation correction in induced pluripotent stem cell (iPSC) derived from recessive dystrophic epidermolysis bullosa (RDEB) using the CRISPR/Cas9 and piggyBac transposon system. J. Dermatol. Sci. *98*, 163–172.
52. Bonafont, J., Mencía, A., Chacón-Solano, E., Srifa, W., Vaidyanathan, S., Romano, R., Garcia, M., Hervás-Salcedo, R., Ugalde, L., Duarte, B., et al. (2021). Correction of recessive dystrophic epidermolysis bullosa by homology-directed repair-mediated genome editing. Mol. Ther. Published online February 18, 2021. https://doi.org/10.1016/j.ymthe.2021.02.019.
53. Tsai, S.Q., Zheng, Z., Nguyen, N.T., Liebers, M., Topkar, V.V., Thapar, V., Wyvekens, N., Khayter, C., Iafrate, A.J., Le, L.P., et al. (2015). GUIDE-seq enables genome-wide profiling of off-target cleavage by CRISPR-Cas nucleases. Nat. Biotechnol. *33*, 187–197.
54. Tsai, S.Q., Nguyen, N.T., Malagon-Lopez, J., Topkar, V.V., Aryee, M.J., and Joung, J.K. (2017). CIRCLE-seq: a highly sensitive in vitro screen for genome-wide CRISPR-Cas9 nuclease off-targets. Nat. Methods *14*, 607–614.
55. Frock, R.L., Hu, J., Meyers, R.M., Ho, Y.J., Kii, E., and Alt, F.W. (2015). Genome-wide detection of DNA double-stranded breaks induced by engineered nucleases. Nat. Biotechnol. *33*, 179–186.
56. Turchiano, G., Andrieux, G., Klermund, J., Blattner, G., Pennucci, V., El Gaz, M., Monaco, G., Poddar, S., Mussolino, C., Cornu, T.I., et al. (2021). Quantitative evaluation of chromosomal rearrangements in gene-edited human stem cells by CAST-Seq. Cell Stem Cell. Published online February 18, 2021. https://doi.org/10.1016/j.stem.2021.02.002.
57. Kern, J.S., Loeckermann, S., Fritsch, A., Hausser, I., Roth, W., Magin, T.M., Mack, C., Müller, M.L., Paul, O., Ruther, P., and Bruckner-Tuderman, L. (2009). Mechanisms of fibroblast cell therapy for dystrophic epidermolysis bullosa: high stability of collagen VII favors long-term skin integrity. Mol. Ther. *17*, 1605–1615.
58. Schwieger-Briel, A., Weibel, L., Chmel, N., Leppert, J., Kernland-Lang, K., Grüninger, G., and Has, C. (2015). A COL7A1 variant leading to in-frame skipping of exon 15 attenuates disease severity in recessive dystrophic epidermolysis bullosa. Br. J. Dermatol. *173*, 1308–1311.
59. March, O.P., Lettner, T., Klausegger, A., Ablinger, M., Kocher, T., Hainzl, S., Peking, P., Lackner, N., Rajan, N., Hofbauer, J.P., et al. (2019). Gene Editing-Mediated Disruption of Epidermolytic Ichthyosis-Associated KRT10 Alleles Restores Filament Stability in Keratinocytes. J. Invest. Dermatol. *139*, 1699–1710.e6.
60. Choi, M., and Lee, C. (2015). Immortalization of Primary Keratinocytes and Its Application to Skin Research. Biomol. Ther. (Seoul) *23*, 391–399.
61. Bornert, O., Kocher, T., Gretzmeier, C., Liemberger, B., Hainzl, S., Koller, U., and Nyström, A. (2019). Generation of rabbit polyclonal human and murine collagen VII monospecific antibodies: A useful tool for dystrophic epidermolysis bullosa therapy studies. Matrix Biol Plus *4*, 100017.
62. Brinkman, E.K., Chen, T., Amendola, M., and van Steensel, B. (2014). Easy quantitative assessment of genome editing by sequence trace decomposition. Nucleic Acids Res. *42*, e168.
63. Clement, K., Rees, H., Canver, M.C., Gehrke, J.M., Farouni, R., Hsu, J.Y., Cole, M.A., Liu, D.R., Joung, J.K., Bauer, D.E., and Pinello, L. (2019). CRISPResso2 provides accurate and rapid genome editing sequence analysis. Nat. Biotechnol. *37*, 224–226.
64. Park, J., Lim, K., Kim, J.S., and Bae, S. (2017). Cas-analyzer: an online tool for assessing genome editing results using NGS data. Bioinformatics *33*, 286–288.